P4.4 ON THE GENESIS AND STRENGTH OF MESOVORTICES FORMED WITHIN BOW ECHOES

Nolan T. Atkins
Lyndon State College, Lyndonville, Vermont

1. INTRODUCTION

Recent numerical and observational studies (Trapp and Weisman 2003; Atkins et al. 2004; Atkins et al. 2005; Wakimoto et al. 2006; Wheatley et al. 2006) of bow echoes have highlighted the important role that small-scale (1-10 km), low-level (0-3 km) "mesovortices" formed on the gust front play in the production of damaging surface winds within bow echoes. It has been shown that mesovortices are capable of producing long, narrow straight-line wind damage swaths that were often thought to be created by the descending rear inflow jet (RIJ). Mesovortices also serve as the parent circulations for tornadoes formed within bow echoes.

Our knowledge of how mesovortices form is based on the analysis of idealized bow echo simulations by Trapp and Weisman (2003). They deduced that mesovortices are created by the tilting of cross-wise horizontal vorticity by convective-scale downdrafts, thus initially producing vertical vortex pairs. It was also shown that the coriolis acceleration plays an important role in amplifying the positive mesovortices while weakening the negative circulations. Observationally, Wakimoto et al. (2006b) observed cyclonic and anticyclonic vertical vortex couplets along the 5 July 2003 bow echo that were observed with airborne Doppler radar data during the Bow Echo and MCV Experiment (BAMEX). However, they also analyzed a bow echo event formed over Iowa on 24 June 2003 that produced only cyclonic mesovortices. Furthermore, single-Doppler analyses of mesovortices by Funk et al. (1999) and Atkins et al. (2004, 2005) have documented the existence of only cyclonic mesovortices to form within bow echoes. Thus, the generality of the tilting mechanism discussed by Trapp and Weisman (2003) and Wakimoto et al. (2006) is not known and needs to be further investigated.

Observational studies by Funk et al. (1999) and Atkins et al. (2004, 2005) have shown that a spectrum of mesovortex strengths may exist within a given event such that some mesovortices produce damage while others produce no damage at all. Therefore, from a detection and warning perspective, it is important to be able to discriminate between the stronger, damaging mesovortices from the weaker ones. Single Doppler radar studies by Atkins et al. (2004, 2005) have shown that structure and evolution of damaging vortices may be different that for the weaker mesovortices. In particular, the damaging mesovortices tended to be longer lived, deeper, and had stronger rotational velocities. Furthermore, Atkins et al. (2005) showed that the damaging mesovortices would form concurrently with or after the genesis of the RIJ. It was hypothesized that the magnitude and depth of vortex stretching was enhanced along the portion of the gust front affected by the RIJ. The generality of this result is not known. More fundamentally, the processes that govern mesovortex strength are not well understood.

In this study, the Advanced Research Weather Research and Forecasting (ARW) model (Skamarock et al. (2005) has been used to investigate mesovortices formed within simulated bow echoes. In particular, quasi-idealized simulations of the 10 June 2003 event during BAMEX (Atkins et al. 2005) have been performed in order to examine the following two objectives. The first is to better understand the mesovortex genesis mechanism(s). Second, an attempt is made to better understand the dynamical processes that control mesovortex strength. In particular, the hypothesis that the RIJ is increasing the magnitude and depth of vortex stretching for the stronger, damaging vortices will be tested.

2. MODEL FORMULATION AND EXPERIMENTAL DESIGN

In order to adequately simulate the system and sub-system scale features observed within the 10 June bow echo, a nested domain configuration was necessary. An outer 400 km x 400 km domain with 1 km horizontal grid resolution contained a nested 120 km x 140 km grid with 0.33 km horizontal grid resolution centered on the leading edge of the bow echo. The outer domain adequately resolved the system-scale bow echo features such as the book-end vortices and RIJ while the nested domain well-resolved mesovortices formed on the lead-

**Corresponding Author Address*: Dr. Nolan T. Atkins, Department of Meteorology, Lyndon State College, Lyndonville, VT 05851; email: nolan.atkins@lyndonstate.edu

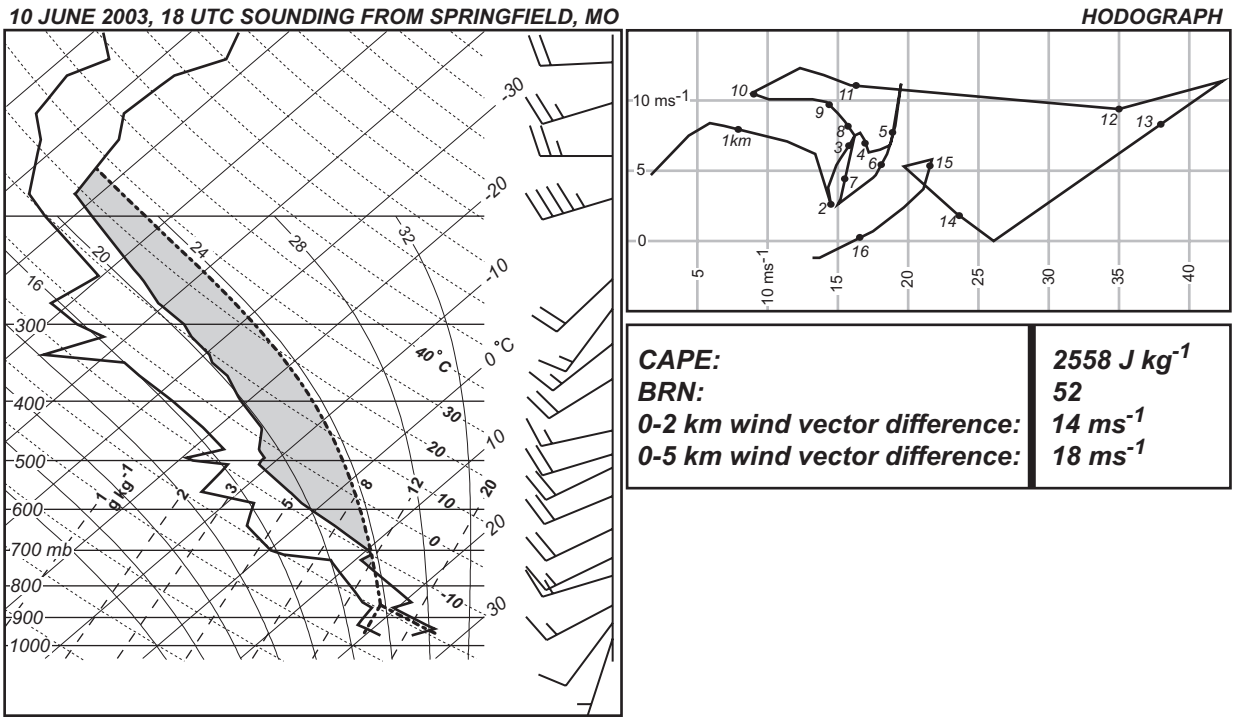

Figure 1. Sounding and hodograph at 1800 UTC from Springfield, MO. Temperature and dewpoint are plotted on the sounding as solid black lines, while a surface-based parcel path is shown as the short-dashed line. The gray area represents the CAPE for the lifted parcel. Winds (half barb = 5 ms^{-1}; full barb = 10 ms^{-1}) are also shown.

ing edge of the bow echo. The vertical grid spacing on both domains varied from 160 m near the surface to 600 m at 17.5 km AGL. The Lin ice scheme was used to parameterize microphysical process on both domains. Turbulence was parameterized with the 1.5 TKE closure scheme and the coriolis force was set to 1x10^{-4} s^{-1}. All simulation were run out for six hours.

The model was initialized with a single sounding from Springfield, Missouri at 18 UTC (Fig. 1). This sounding was launched in a high θ_e air mass that appears to represent the environment that formed the MCS on the afternoon of 10 June over central Missouri. The sounding contained 2558 J kg^{-1} of Convective Available Potential Energy (CAPE) and moderate low-level wind shear (Fig. 1). Convection was initiated with three thermal bubbles spaced 20 km apart in the north-south direction in the center of the domain.

3. BOW ECHO AND MESOVORTEX STRUCTURE

Results from the control simulation are shown in Fig. 2 where data are presented at 4 hours and 20 minutes into the model simulation. In Fig. 2a, data on the coarse domain are shown. One can see in the simulated radar reflectivity and storm-relative wind fields that a well-defined, mature bow echo is present. System-scale freatures such as the book-end vortices and RIJ are observed in the model data. An intense line of leading convective cells and strong reflectivity gradient at the leading edge of the convective system are present. The overall structure and scale of the simulated mature bow echo is qualitatively similar to what was documented by Atkins et al. (2005) for the 10 June 2003 event. Also notice the undulations present along the leading edge of the bow echo. A more detailed depiction of the bow echo gust front is shown on the higher resolution domain in Fig. 2b. One can again see the RIJ impinging upon and diverging at the leading edge of the bow echo. On the bow echo gust front, mesovortices are readily apparent as local maxima in the vertical vorticity field. Notice that the stronger mesovortices appear to be located along the portion of the gust front that has been influenced by the RIJ. The mesovortices also appear to be associated with appendages in the reflectivity field. A more detailed view of a mesovortex can be seen in Fig. 2c. A well-defined closed circulation collocated with a maximum in vertical vorticity and associated with an

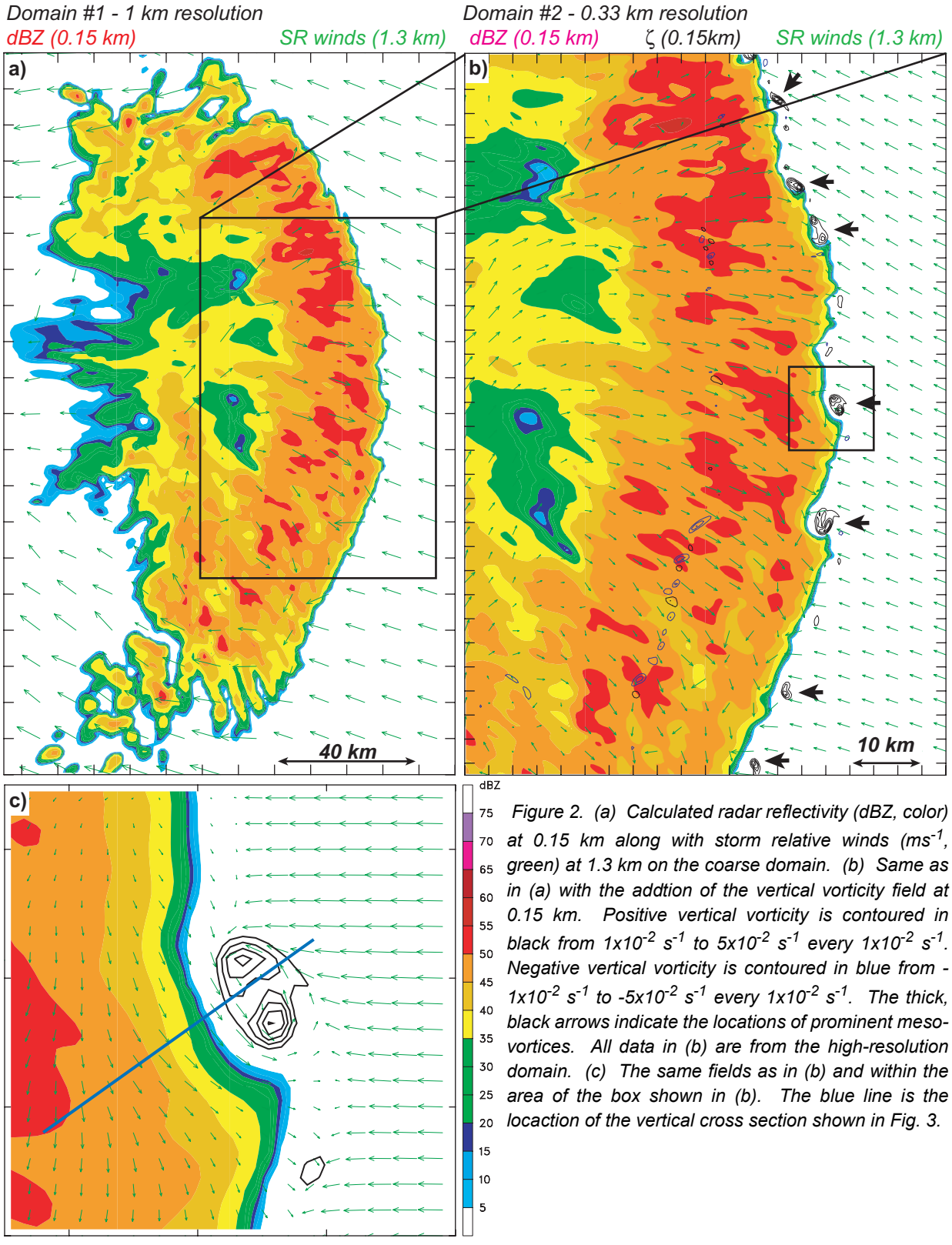

Figure 2. (a) Calculated radar reflectivity (dBZ, color) at 0.15 km along with storm relative winds (ms^{-1}, green) at 1.3 km on the coarse domain. (b) Same as in (a) with the addtion of the vertical vorticity field at 0.15 km. Positive vertical vorticity is contoured in black from $1x10^{-2}$ s^{-1} to $5x10^{-2}$ s^{-1} every $1x10^{-2}$ s^{-1}. Negative vertical vorticity is contoured in blue from $-1x10^{-2}$ s^{-1} to $-5x10^{-2}$ s^{-1} every $1x10^{-2}$ s^{-1}. The thick, black arrows indicate the locations of prominent meso-vortices. All data in (b) are from the high-resolution domain. (c) The same fields as in (b) and within the area of the box shown in (b). The blue line is the locaction of the vertical cross section shown in Fig. 3.

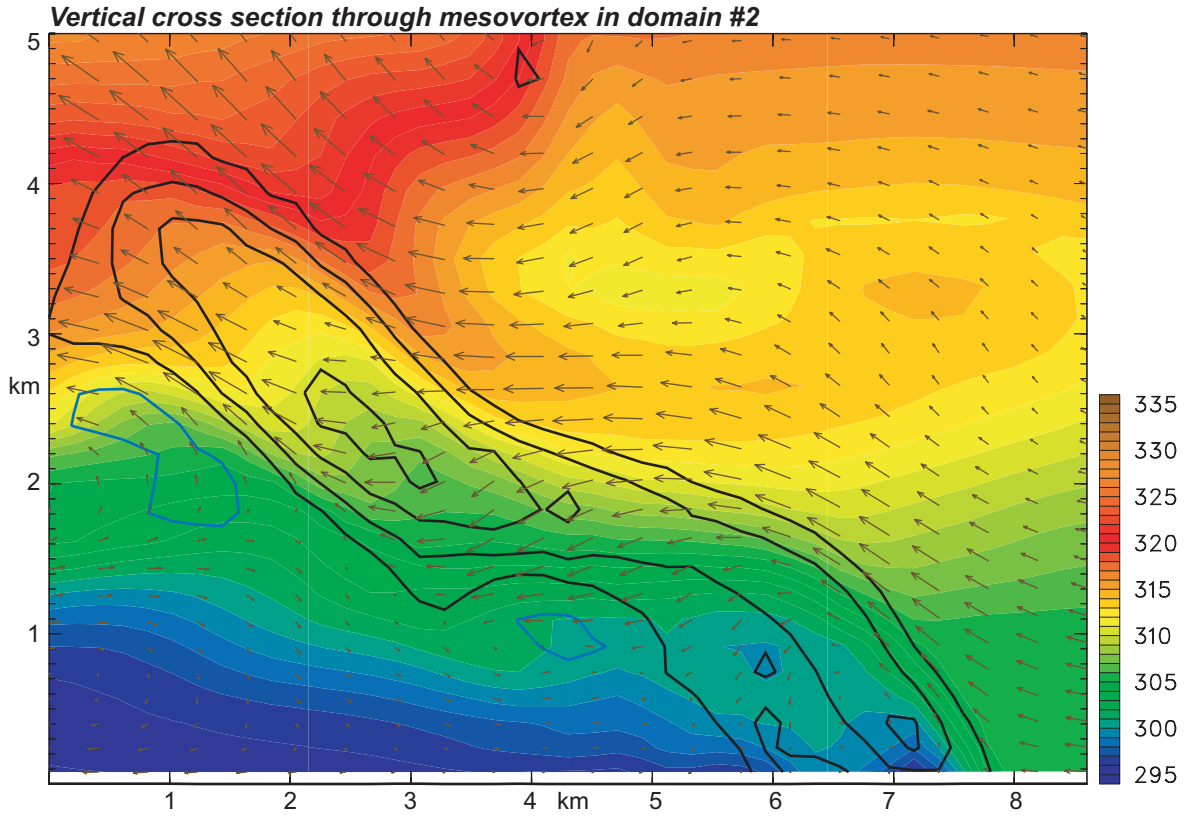

Figure 3. Vertical cross section through the mesovortex shown in Fig. 2c. Potential temperature (K) is plotted in color with the scale to the right of the figure. Vertical vorticity is plotted using the same convention as Fig. 2b. Winds (ms^{-1}) in the plane of the cross section are shown in brown.

appendage in the refectivity field is apparent. It is clear from the results in Fig. 2c that the higher-resolution model domain is able to adequately resolve these small-scale circulations. The minor axis diameter of the mesovortex in Fig. 2c is about 3 km.

The vertical structure of of the vortex in Fig. 2c is shown in Fig. 3. The vortex is clearly tilting rearward along the gust front of the bow echo and is observed up to about 4 km. Notice that at the surface, the vortex appears to be located on the cold-air side of the bow echo gust front.

5. SUMMARY AND FUTURE WORK

Quasi-idealized modeling results of the 10 June 2003 Saint Louis bow have been presented. A portion of the control simulation was presented herein and appears to capture many of the system and subsystem-scale features that were observed with the 10 June event. In particular, the higher-resolution nested domain well-resolves the structure of the mesovortices formed on the leading edge of the bow echo.

Future work will proceed in two areas. First, a number of sensitivity runs are currently being performed to examine how mesovortex formation and evolution is dependent on the coriolis acceleration, cold pool strength, and magnitude of the low-level environmental wind shear. Weisman and Trapp (2003) and Trapp and Weisman (2003) noted that mesovortex evolution is sensitive to the coriolis acceleration and magnitude of the low-level shear value.

Second, future work will examine how these vortices form and the process that are important for their intensification. In particular, the hypothesis that the RIJ increases the depth and magnitude of vortex stretching will be tested.

Acknowledgements: The research results presented herein were supported by the National Science Foundation under Grant ATM-0233178 and Vermont EPSCoR EPS-0236976.

References

Atkins, N.T., J.M. Arnott, R.W. Przybylinski, R.A. Wolf, and B.D. Ketcham, 2004: Vortex structure and evolution within bow echoes. Part I: Single-Doppler and damage analysis of the 29 June 1998 Derecho. *Mon. Wea. Rev.*, **132**, 2224-2242.

_____, C.S. Bouchard, R.W. Przybylinski, R.J.Trapp, and G. Schmocker, 2005: Damaging surface wind mechanism within the 10 June 2003 Saint Louis bow echo during BAMEX. *Mon. Wea. Rev.*, **133**, 2275-2296.

Funk, T. W., Darmofal, K. E., Kirkpatrick, J. D., DeWald, V. L., Przybylinski, R. W., Schmocker, G. K., and Y-J Lin, 1999: Storm reflectivity and mesocyclone evolution associated with the 15 April 1994 squall line over Kentucky and southern Indiana. *Wea. Forecasting,* **14**, 976–993.

Skamarock, W. C., J. B. Klemp, J. Dudia, D. O. Gill, D. M. Barker, W. Wang, and J. G. Powers, 2005: A description of the Advanced Research WRF version 2. NCAR Tech. Note NCAR/TN-468+STR, 100 pp.

Trapp, R.J. and M.L. Weisman, 2003: Low-level mesovortices within squall lines and bow echoes. Part II: Their genesis and implications. *Mon. Wea. Rev.*, **131**, 2804-2823.

Wakimoto, R.M., H.V. Murphy, C.A. Davis, and N.T. Atkins, 2006: High winds generated by bow echoes. Part II: The relationship between the mesovortices and damaging straight-line winds. Accepted to *Mon. Wea. Rev.*

Weisman, M.L., and R. J. Trapp, 2003: Low-level mesovortices within squall lines and bow echoes: Part I. Overview and dependence on environmental shear. *Mon. Wea. Rev.*, **131**, 2779-2803.

Wheatley, D.M., R.J. Trapp, and N.T. Atkins, 2006: Radar and damage analysis of severe bow echoes observed during BAMEX. *Mon. Wea. Rev.*, **134**, 791-806.